RSC Advances

PAPER

View Article Online
View Journal | View Issue

Cite this: *RSC Adv.*, 2022, **12**, 9637

Open-tubular capillary electrochromatography with hydroxypropyl-β-cyclodextrin imprinted polymers: hybrid polyhedral oligomeric silsesquioxane as a coating for enantioseparation

Jian Zhang,[ab] Lingling Liang,[ab] Yanqing Miao,[ab] Yang Yang,[a] Xin Bao[a] and Chunye Liu *[ab]

Received 6th January 2022
Accepted 22nd March 2022

DOI: 10.1039/d2ra00079b

rsc.li/rsc-advances

A hydroxypropyl-β-cyclodextrin (HP-β-CD) imprinted coating based on polyhedral oligomeric silsesquioxane (POSS) for open tubular electrochromatography was prepared. The mixture of methacryl-POSS (MA0735), HP-β-CD (template), methacrylic acid (MAA, monomer), *N*,*N*′-methylenebisacrylamide (MBA, crosslinker) and toluene-dimethyl sulfoxide (porogen) was used to synthesize the chiral selective coating. The influence of synthesis parameters on the imprinting effect and separation performance, including the amount of HP-β-CD, POSS, and MAA, was investigated systemically. The optimum polymerization was prepared by mixing HP-β-CD, MA0735, MAA, and MBA with the molar ratio of 1 : 1.87 : 1.60 : 1.60. Five racemates were separated by the modified capillary columns using aqueous buffer. Column efficiency on the POSS-based MIPs coating column was greater than 22 000 plates/m. MIPs-POSS hybrid coating capillaries had improved resolution (3.36 times) and the greatest resolution was up to 6.15 within 10 min.

1. Introduction

About half of drugs are chiral compounds and only about 25% are administered as pure enantiomers.[1] In most cases, the pharmacological activity is restricted to one of the enantiomers, whereas the other often causes side effects. Meanwhile, enantiomers of amino acids often show different physiological activities. Therefore, chiral separation has attracted extensive attention.[2,3] In various chiral separation methods, capillary electrophoresis (CE) is a powerful technology owing to its simplicity, high efficiency, low cost, and the flexibility of separation mode.[4–6] Open-tubular capillary electrochromatography (OT-CEC) is one of the CE modes that is widely applied for chiral separation.[7–9] In OT-CEC, the stationary phase is coated onto the inner wall of a capillary through polymer coatings, porous silica layers, etching and sol gel technology.[7] Among these types, polymer coating provides a better alternative because of its long-term stability.[7,8]

Molecularly imprinted polymers (MIPs) are ideal polymeric materials. The template-based synthesis makes them have tailor-made recognition sites and high selectivity with the memory of shape, size and three-dimensional complementary cavities of template molecule.[10] High selectivity, identification, sensitivity, low cost and easy preparation make MIPS have attracted great attention in the fields of purification and selective separation.[11–14] MIPs have been used as stationary phases in OT-CEC.[15–18] In spite of successful separation achieved, MIPs may suffer from shrinking or swelling when exposed to different solvents.[19] The silica-based MIPs solve this problem partially. However, the low tolerance to pH value often limits their use.[20] Thus, organic–inorganic hybrid MIPs are applied to overcome the problem because they combine the merits of the organic polymer and inorganic materials.[21–23] Polyhedral oligomeric silsesquioxanes (POSS) is a kind of cagelike silsesquioxane with the formula $(RSiO_{1.5})_n$, which embody organic–inorganic cage like architecture containing an inner inorganic framework made up of silicon and oxygen.[24] POSS has many advantages such as facile chemical modification, good pH tolerance, high temperature and oxidation resistance.[24,25] Furthermore, POSS materials are thought as the truly molecularly dispersed nanocomposites, which can be easily incorporated into common polymers *via* copolymerization, grafting or blending. POSS, POSS based ionic liquid, and MIPs hybrid POSS polymer have been well used in CEC separation as packed or open-tubular stationary phases.[26–30] POSS-containing monomers contribute rigid skeleton for capillary stationary and improve the separation of analytes. However, to best of our knowledge, few studies about MIPs-POSS coating capillary for enantioseparation both of amino acids and drugs have been reported to date.

[a]*School of Pharmacy, Xi'an Medical University, Xi'an 710021, China. E-mail: doris8976@163.com*
[b]*Institute of Medicine, Xi'an Medical University, Xi'an 710021, China*

Herein, POSS based MIPs open-tubular capillaries for CEC using POSS MA0735 as the network and hydroxypropyl-β-cyclodextrin (HP-β-CD) as the template were prepared for the first time. POSS MA 0735 has eight organic methacrylate groups attached at the corners of the cage, which can form hybrid polymers. HP-β-CD is a widely used chiral selector because of its multiple chiral centers.[31–34] Furthermore, it possesses numerous functional groups that allow it to have multiple interactions with functional monomer through hydrogen bonding, charge–charge, hydrophobic, and steric interactions. The strong enough interaction between template molecules and functional monomers will be beneficial to improve the selectivity and recognition ability of MIPs.[35] The effects of the polymerization mixture composition and separation conditions on the ability of enantiomer separation were investigated systemically.

2. Materials and methods

2.1 Apparatus

All CE experiments were carried out on a Beckman P/ACE MDQ capillary electrophoresis system equipped with an on-column UV detector, an auto-sampler, and a liquid temperature control system (Beckman Kurt Trading Co., Ltd, USA). The fused silica capillary, with dimensions of 75 μm i.d. (375 μm o.d.) × 60.0 cm (50.0 cm to detection window), was purchased from Yongnian Reafine Chromatogram Equipment Co., Ltd (Hebei, China). Infrared spectra were recorded on a Tensor 27 infrared spectrometry (Bruker, Germany). The micrographs with a thin layer of gold were taken by SEM (VEGA II, TESCAN, Czech Republic). The calculation of the pore size and surface area were performed using TriStar II 3020 surface area and porosity system (Micromeritics, US). The X-ray photoelectron spectroscopy (XPS) analysis was taken by AXIS Supra instrument (Shimadzu, Japan). Thermogravimetric analysis (TGA) was carried out using a STA 409 PC thermal gravimetric analyzer (Netzsch, Germany). X-ray diffraction (XRD) patterns of the samples were obtained with a DMAX-3CX X-ray diffractometer (Rigaku, Japan).

2.2 Chemicals and reagents

3-(Trimethoxysilyl)propyl methacrylate (γ-MPS, ≥99.0%), methacrylic acid (MAA, AR grade), DL-tyrosine (DL-Tyr), DL-phenylalanine (DL-Phe), DL-tryptophan (DL-Trp), DL-histidine (DL-His) were all from Shanghai Aladdin Biochemical Technology Co., Ltd (Shanghai, China). Methacryl POSS (POSS-MA0735, ≥90.0%) was obtained from Changsha Baxi Co., Ltd (Hunan, China). Hydroxypropyl-β-cyclodextrin (HP-β-CD) was obtained from Shanghai San Chemical Technology Co., Ltd (Shanghai, China). *N*,*N*′-Methylenebisacrylamide (MBA) was from Tianjin Fuchen Chemical (Tianjin, China). Azobisisobutyronitrile (AIBN, ≥99.0%) was purchased from Shanghai Aibi Chemical Technology Co., Ltd (Shanghai, China). Acetonitrile (ACN, HPLC grade) was obtained from Tianjin Tianli Chemical Co., Ltd (Tianjin, China). Isoprenaline hydrochloride injection (0.5 mg mL^{-1}, racemic samples) was from Shanghai Hefeng Pharmaceutical Co., Ltd (Shanghai, China). Ephedrine standard was provided by College of Chemistry and Materials Science, Northwestern University (Xi'an, China). Dimethyl sulfoxide (DMSO, ≥99.5%) was from Tianjin Xuan'ang Science Industry and Trade Co., Ltd (Tianjin, China). All the reagents were analytical grade unless otherwise stated.

2.3 Preparation of MIPs-POSS coating capillary

A bare fused-silica capillary was flushed successively with 1 M NaOH, deionized water, 1 M HCl, and deionized water for 30, 15, 15, and 15 min, respectively, and dried with N_2 gas. Then the capillary was filled with γ-MPS acetone solution (5/5, v/v), sealed at two ends with rubber septa, activated in a 50 °C water bath for 1.5 h. The capillary was then rinsed sequentially by acetone and water, and finally dried with N_2 gas. HP-β-CD (0.0288 mmol, template molecule), methacryl POSS (0.1347 mmol), MAA (0.1153 mmol, functional monomer) were dissolved in 600 μL toluene-DMSO (3/7, v/v). And then the pre-polymerization mixture was sonicated for 15 min. Then, 11.4 mg AIBN and 0.1153 mmol MBA were dissolved in 400 μL toluene-DMSO (3/7, v/v). After that, it was dispersed into the pre-polymer solution and introduced into the capillary using a syringe. The capillary was sealed at both ends again and reacted for 12 h at room temperature and incubated in a 50 °C water bath for 30 min. After polymerization, the capillary was flushed with acetonitrile and methanol/acetic acid (9/1, v/v) using vacuum pump to remove the unreacted mixture and the imprinted molecules, respectively.[29] Recipes of POSS based MIP capillary coatings was shown in Table 1. The MIPs capillary column without POSS materials were prepared using the same procedure but without addition of POSS. For the scanning electron microscopic test, the polyimide coating on the outer wall of the capillary was scraped off and MIPs-POSS coating process was conducted.

2.4 CEC conditions

For CEC separations, the electrolyte used was 20 mmol L^{-1} phosphate buffers (pH 7.4, unless otherwise stated). The samples were injected into the capillaries by the pressure injection mode at 0.5 psi for 3 s. The separation voltage was 20 kV, unless otherwise stated. UV detection was performed at 214 nm. A detection window was created at a distance about 10 cm from the outlet end of the capillary by removing 2–3 mm length of the polyimide coating. Between two runs, the capillary must be rinsed sequentially with deionized water and buffer solution for 3 min, respectively. Deionized water was used in all the experiments. All the solutions were stored in the refrigerator at 4 °C, and filtered with 0.45 μm pore membrane filters and degassed by sonication prior to use.

3. Results and discussion

3.1 Characterization of MIPs-POSS coating

Schematic representation of the preparation process of MIPs-POSS coating column was shown in Fig. 1. Infrared spectrum is a direct way to clarify the existence of functional group on the MIPs-POSS coating. The FT-IR results (Fig. 2) showed that POSS-

Table 1 Recipes of POSS based MIP capillary coatings

Capillaries	HP-β-CD (mmol)	MA0732 (mmol)	MAA (mmol)	MBA (mmol)	AIBN (mg)	Toluene (μL)	DMSO (μL)
c1	0.0288	0.1347	0.1153	0.1153	11.4	300	700
c2	0.0576	0.1347	0.1153	0.1153	11.4	300	700
c3	0.072	0.1347	0.1153	0.1153	11.4	300	700
c4	0.0864	0.1347	0.1153	0.1153	11.4	300	700
c5	0.144	0.1347	0.1153	0.1153	11.4	300	700
c6	0.288	0.1347	0.1153	0.1153	11.4	300	700
c7	0.072	0	0.1153	0.1153	11.4	300	700
c8	0.072	0.2020	0.1153	0.1153	11.4	300	700
c9	0.072	0.2694	0.1153	0.1153	11.4	300	700
c10	0.072	0.3368	0.1153	0.1153	11.4	300	700
c11	0.072	0.4041	0.1153	0.1153	11.4	300	700

based MIP (asymmetric *n*Si–O–Si) has a very strong absorption band at 1145.67 cm^{-1}, which indicates that POSS groups have been successfully integrated into MIP matrix. The strong absorption peak of about 3400 cm^{-1} was characteristic for hydroxyl (O–H) absorption. The absorption peaks at 2929.52 cm^{-1} and 1388.69 cm^{-1} represent the stretching vibration and in-plane bending vibration of methyl (C–H) for MAA, respectively. Besides, the stretching signal for C=O group (1728.15 cm^{-1}) could be found in infrared spectra of hybrid column, indicating the immobilization of POSS backbone. Comparatively, there was not the absorption at opposite wave number in the FT-IR spectrum of bare silica capillary.

In addition to FT-IR, XPS, SEM, XRD, TGA, and N_2 adsorption–desorption experiments were employed to characterize the MIPs-POSS coating. The XPS spectra (Fig. 3) show that the coating material contains elements C, Si, O and N, indicating that POSS has been hybridized into the polymer. XPS analysis of C binding configurations finds carbon with carbonyl (C=O)[36] (peak at 287.3 eV) in the coating material, which is consistent with the FT-IR results.

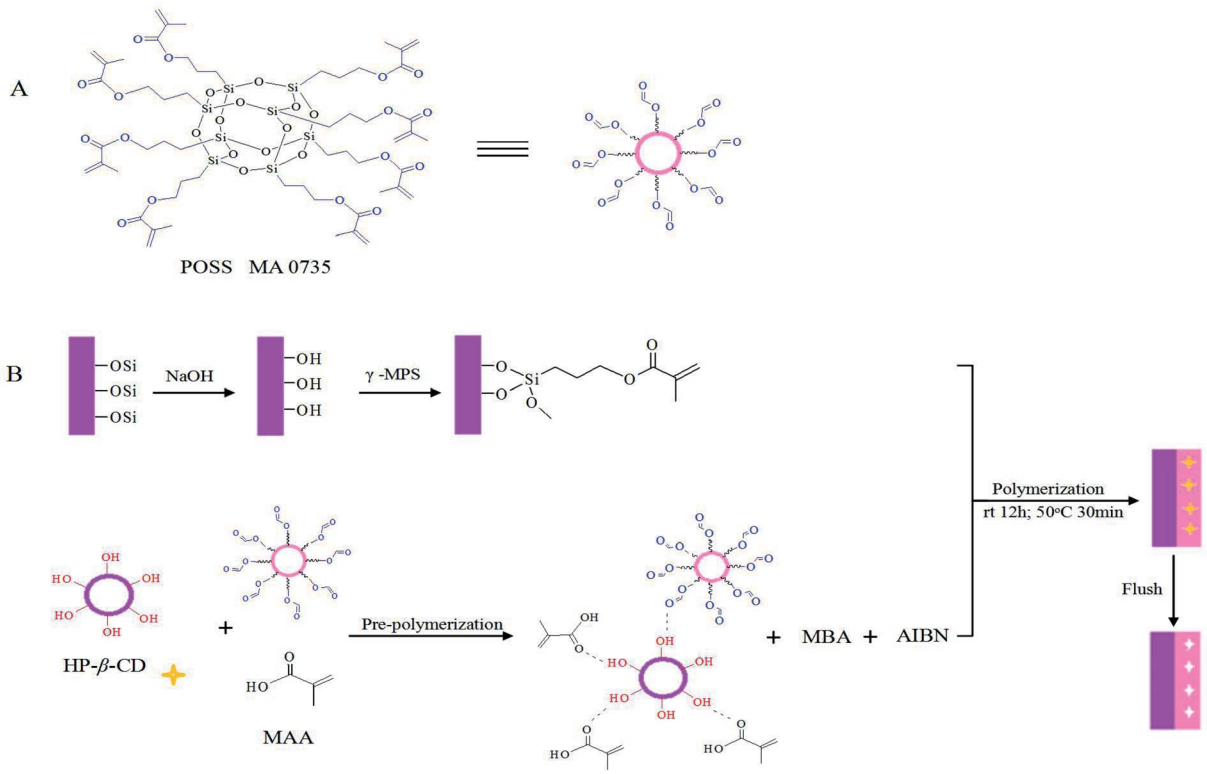

Fig. 1 (A) Structure of POSS MA 0735 and (B) schematic representation of the preparation process of POSS-MIPs column. Herein, HP-β-CD, MAA, MBA, and toluene-dimethyl sulfoxide were used as template, monomer, crosslinker, and porogen, respectively. In the pre-polymerization, there was a strong enough interaction between HP-β-CD, MAA, and POSS. After adding of AIBN (initiator) and MBA (crosslinker), the polymerization took place. After the reaction, unreacted reagents and templates were removed by acetonitrile and methanol/acetic acid (9/1, v/v), respectively.

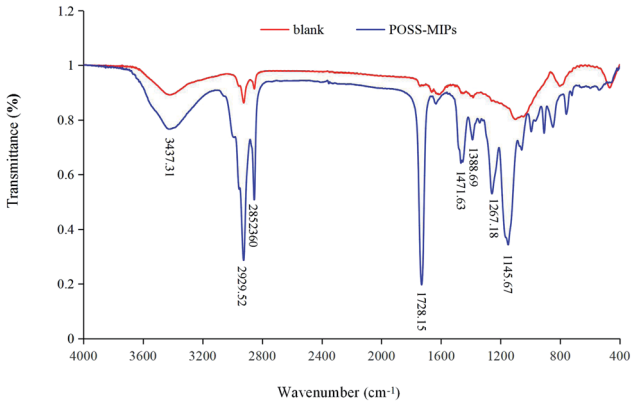

Fig. 2 FT-IR spectra of POSS-MIPs coating column (blue line) and blank fused silica capillary column (red line).

Fig. 4A shows microstructure of the POSS-based films on capillary segments. Through SEM investigations, the morphology of a porous polymer layer tightly coated onto the prepared column could be seen. N_2 adsorption–desorption studies reveals an average pore width of 4.07 nm, pore volume of 0.595 $cm^3\ g^{-1}$, and surface area of 583.68 $m^2\ g^{-1}$. Fig. 4B shows incomplete type IV of N_2 adsorption–desorption isotherms with type H4 hysteresis loops, suggesting narrow slit-like pores. The XRD pattern of MIPs-POSS material shows no sharp peak (Fig. 4C), indicating that the coating has an amorphous structure. While, the broad peak at $2\theta = 20°$ was observed, which may correspond to amorphous Si compounds.[37] Due to the limitation of the TGA instrument, the temperature only rises to 500 °C in analysis. However, Fig. 4D still partially shows the thermal properties of the coating material. A major mass loss (55%) took place between 300 and 450 °C, mostly because of the intensive pyrolysis of the poly(-methacrylic anhydride) backbone chains.[38] Different from the curve of pure PMAA,[38] the material has not been completely decomposed at 500 °C (40% residual), indicating the existing of POSS in the polymer coating.

3.2 Effects of HP-β-CD content

It has been reported that better sufficient EOF in CEC can be obtained by using MAA as functional monomer,[39] so MAA was selected in the study. In order to dissolve enough POSS and improve the affinity of the final MIP membrane, the binary porogen toluene/DMSO was used after comparing ACN/toluene, ACN/DMSO and toluene/DMSO. To obtain a non-covalent imprinted polymer with good recognition performance, the interaction degree between template molecules and functional monomers before polymerization is a crucial factor.[40] Therefore, the molar ratio of template-functional monomer was a key factor in imprinting process. Varying the molar ratio of functional monomer MAA to the template molecule was performed by adjusting the amount of HP-β-CD molecule added to an otherwise constant prepolymerization mixture (Table 1, c1–c6). EOF was detected using DMSO (0.2%) as a marker, and the

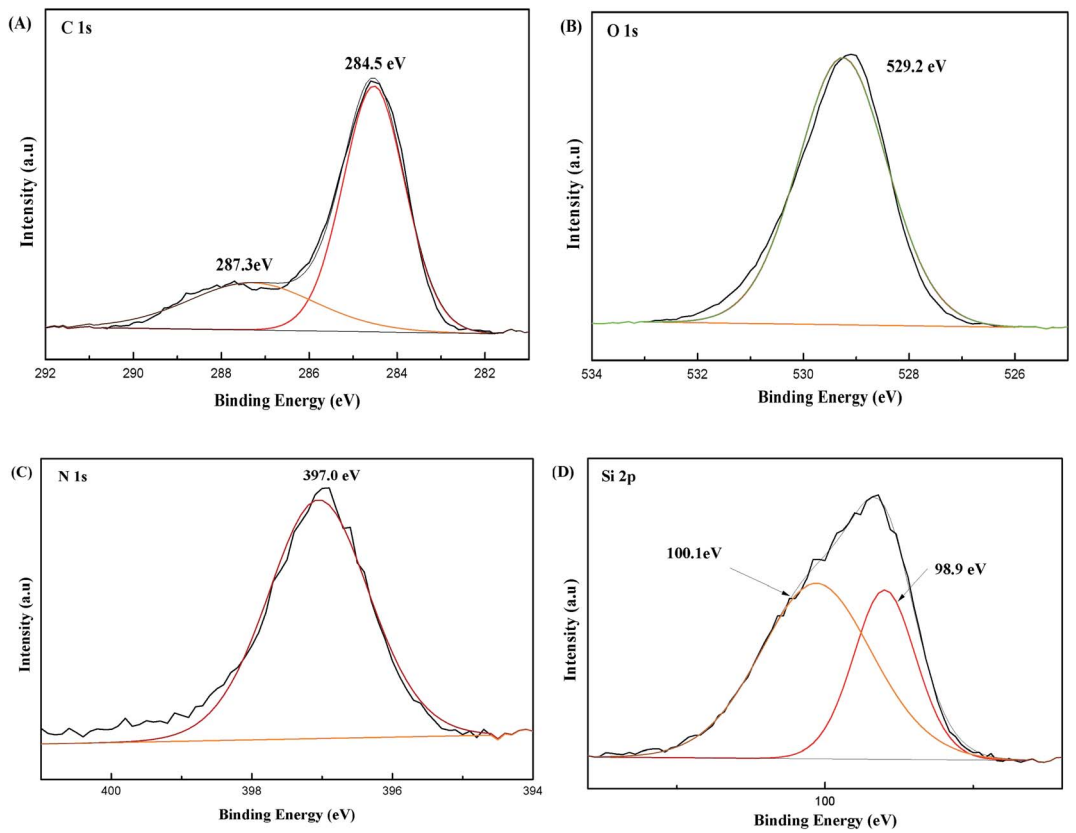

Fig. 3 X-ray photoelectron spectroscopy (XPS) spectra of MIPs-POSS coating material (C3).

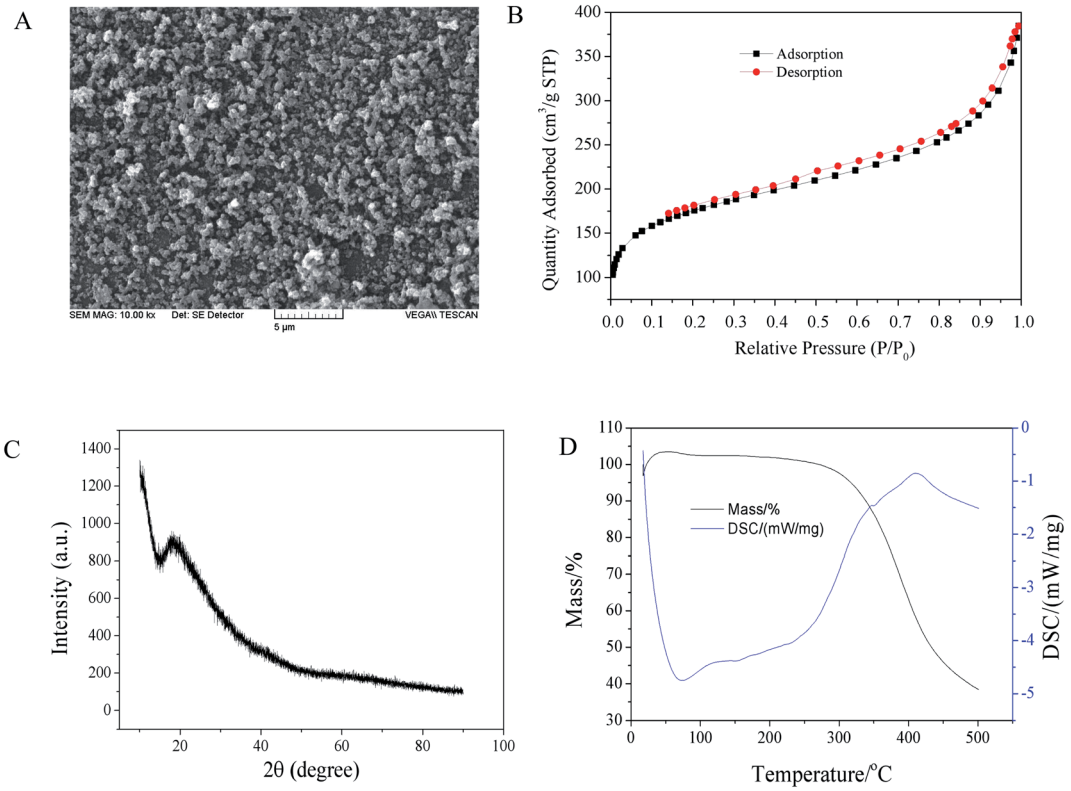

Fig. 4 SEM photo (A), N_2 adsorption–desorption isotherms (B), XRD pattern (C), and TGA curve of MIPs-POSS coating (C3).

electrophoretic conditions were given in Section 2.4. The results showed that EOF decreased with the increasing of HP-β-CD content, and reached the minimum at c4 column (Fig. 5A). The low migration speed can prolong the residence time of the substance in the capillary column, which is benefit to chiral recognition. The EOF of c3 to c7 columns was sufficient for separation. DL-His, DL-Phe, DL-Tyr, and DL-Trp were all partially separated in c3 column. Partial separations were also achieved in columns c2, c5, and c6 (Fig. 5B). The column performance for His on c3 was best (118 748 plates/m). According to the results, c3 (0.072 mmol HP-β-CD, 0.1153 mmol MAA) column was selected to optimize the experimental conditions.

3.3 Effects of POSS content

The effect of POSS amount on the EOF and separation was further investigated to understand the function of POSS. The hydrophobicity inside the POSS-based MIPs significantly depend on the monomer concentrations in the reaction solutions.[25] The percent of POSS monomers was adjusted by changing the amount of POSS at a fixed amount of MAA (Table 1, c3, c7–c11). The results indicated that EOF of c3, c10 and c11 columns was small (Fig. 5C), which is beneficial to chiral separation. However, it is easy to cause failure of column preparation in c10 and c11 because of the high viscosity of POSS. Moreover, higher POSS content lead to electrophoresis baseline instability, which may be due to the non-uniform bonding of polymers on the inner wall of the column caused by the hydrophobicity of POSS. As shown in Fig. 5D, DL-His, DL-Phe, DL-Tyr, DL-Trp, and DL-Dopa were all get part separation, and the enantiomeric selectivity of POSS-based MIPs column was significantly higher than POSS-free one (c7). For example, resolution (R_s) of DL-His on POSS-based MIPs column (c3) was 3.36 times of that on POSS-free one (c7).

3.4 Effects of polymerization time

Polymerization time is a key factor to control the characteristics of MIP coatings, such as layer thickness and porosity. Generally, the specific surface area of MIP monolith will decrease with the polymerization time. The effect of heating time on enantiomeric selectivity was investigated by using c3 column and heating in water bath at 50 °C. As shown in Fig. 6A, the resolution of DL-His increased significantly with the prolongation of heating time, and the optimum heating time is 30 minutes (R_s was 1.52, column performance of first peak was 125 335/m and second peak was 92 004/m, respectively). However, further increasing polymerization time lead to a blocked capillary. So, the polymerization time was fixed at 30 min in the study.

3.5 Effects of CEC conditions

For a MIPs-POSS column, the chiral recognition ability is also affected by electrophoresis conditions. Buffer pH can determine charge state of analytes and the polymer surface. As shown in Fig. 6B, the separation of DL-His (in c3 columns) was improved significantly with the increasing of pH and achieved efficient separation at pH 7.4 (R_s was 1.52, column performance of first

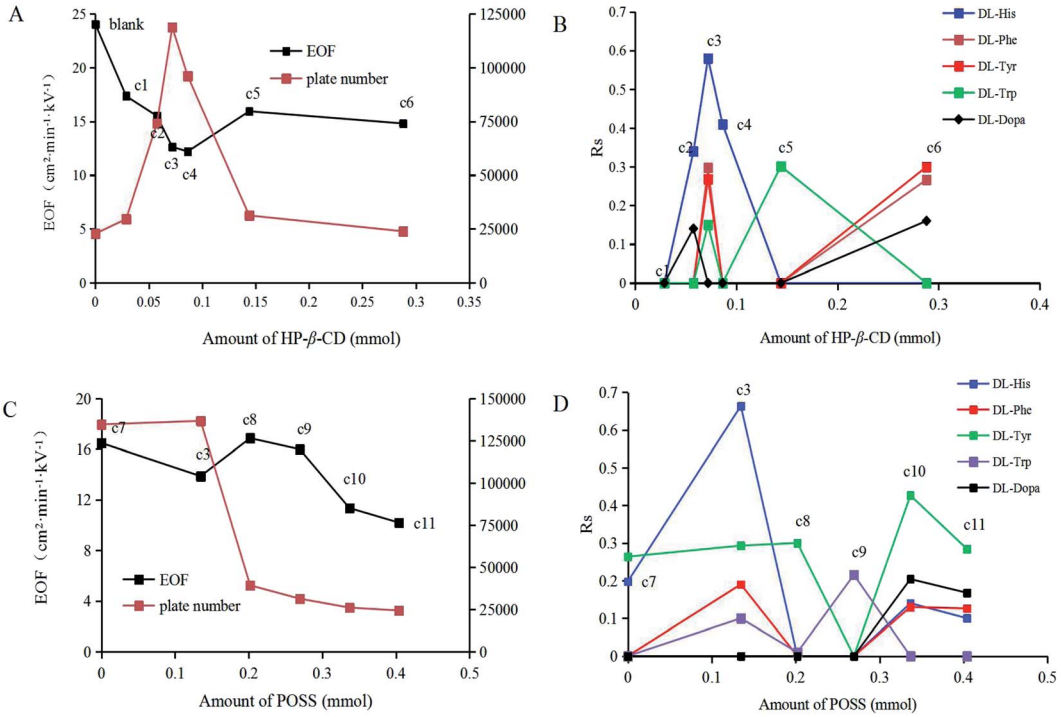

Fig. 5 (A) Effects of HP-β-CD amount on EOF and plate number, (B) effects of HP-β-CD amount on separation resolution of analytes, (C) effects of POSS amount on EOF and plate number, and (D) effects of POSS amount on resolution of analysts.

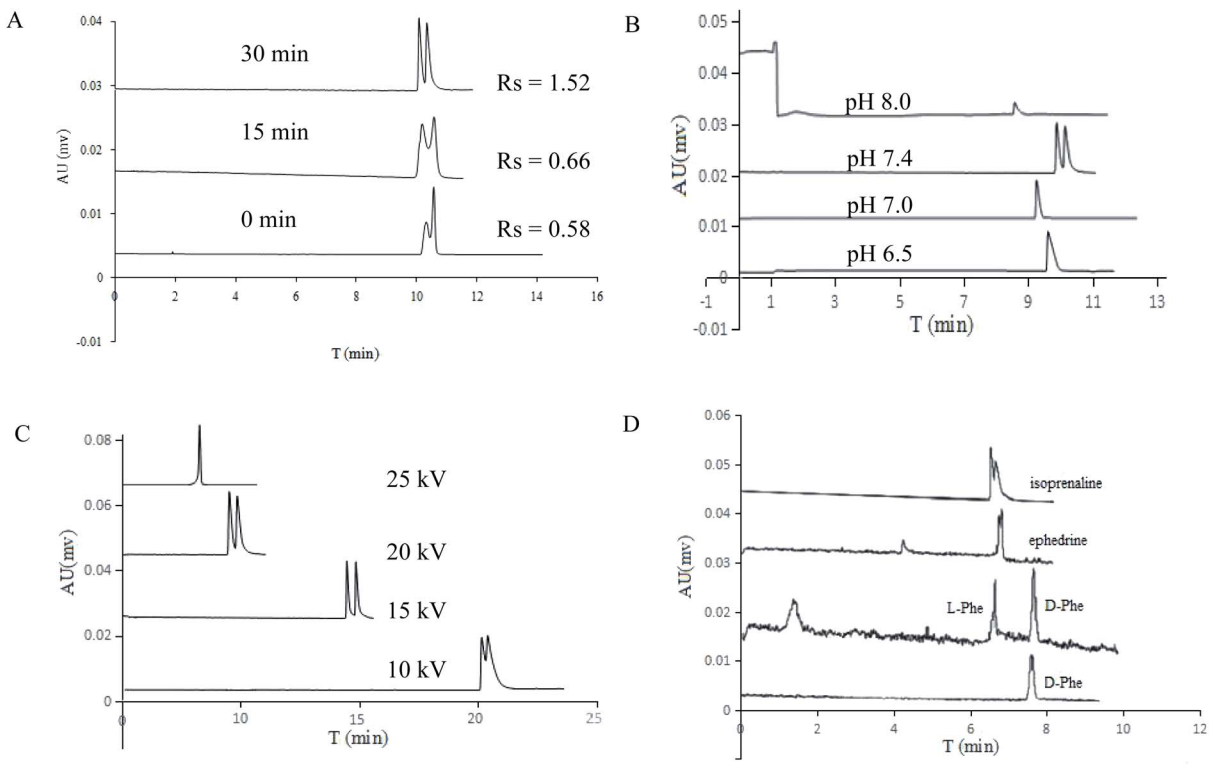

Fig. 6 Electropherograms of DL-His on c3 column with different polymerization time (A), with different buffer pH (B), with different voltage (C), and (D) electropherograms of other racemates on c3 column. Conditions: (A) separation voltage, 20 kV; buffer, 20 mmol L^{-1} phosphate (pH 7.4), (B) separation voltage, 20 kV; buffer, 20 mmol L^{-1} phosphate (pH 6.5–8.0), (C) separation voltage, 10–25 kV; buffer, 20 mmol L^{-1} phosphate (pH 7.4), and (D) separation voltage, 15 kV; buffer, 20 mmol L^{-1} phosphate (pH 7.4). Other conditions were all same, such as capillary, 75 μm i.d. (375 μm o.d.), 60.0 cm total length and 50.0 cm effective length; detection wavelength, 214 nm; injection, 0.5 psi × 3 s.

peak was 125 335/m and second one was 92 004/m). Generally, the operating voltage will affect the interaction time between enantiomers and chiral selector, and intrinsically affects the resolution. The effect of operating voltage on the DL-His separation was investigated in the range of 10–25 kV in the study. As shown in Fig. 6C, the retention time of DL-His decreased with the increasing voltage. Its baseline separation was obtained when the voltage was 15 kV (R_s was 1.65, column performance of first peak was 96 146/m and the second one was 78 929/m). With the further increasing of voltage, the resolution and column performance decreased.

3.6 Stability and reproducibility of the MIPs-POSS coating capillaries

The stability and reproducibility of the MIPs-POSS coating columns (c3) were tested by measuring the separation of DL-His racemates. The relative standard deviation (RSD) of inter-capillary and intra-capillary reproducibility for the resolution of two enantiomers (DL-His) on the MIPs-POSS capillary was lower than 5% (Table 2). The chromatographic behavior of DL-His compared with the beginning of a new column and after 200 injections (R_s was 1.56, column performance of first peak was 93 552/m and the second one was 76 334/m), no untoward changes were observed in the chromatograms (Fig. 7). In addition to amino acids enantiomers, POSS-based MIPs capillary has potential on racemate drugs separation, such as ephedrine and isoprenaline hydrochloride (Fig. 6D). For DL-Phe, the baseline separation was obtained within 10 min. R_s was 6.15, column performance of L-Phe and D-Phe were 141 653/m and 44 480/m, respectively. For ephedrine and isoprenaline hydrochloride, the column performances were all higher than 22 000/m and the separation were completed in 10 min.

Table 2 The reproducibility (RSD%) on POSS-based capillaries with HP-β-CD imprints (C3) of inter-capillary and intra-capillary

Parameter	Inter-capillary	Intra-capillary
t_1	1.9	4.9
t_2	2.5	4.8
α	0.6	0.2
N_1	3.8	4.5
N_2	3.6	4.3
R_s	3.3	4.0

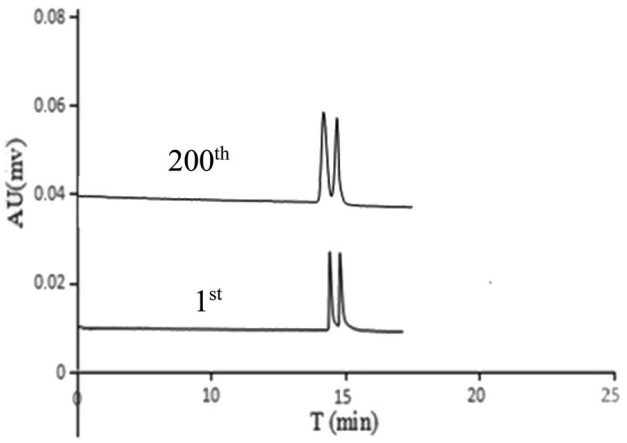

Fig. 7 Electropherograms of DL-His on c3 column of the 1st and 200th running. Conditions: capillary, 75 μm i.d. (375 μm o.d.), 60.0 cm total length and 50.0 cm effective length; separation voltage, 15 kV; detection wavelength, 214 nm; injection, 0.5 psi × 3 s; buffer, 20 mmol L^{-1} phosphate (pH 7.4).

4. Conclusion

In the study, new MIPs-POSS coating capillaries were synthesized. Eight organic methacrylate groups of POSS MA0735 make the polymerization more efficient. As a powerful chiral selector, HP-β-CD was used as imprinting molecule to increase the selectivity of the column. Different with the literature,[21,27,28] the buffer used in this study did not contain organic reagents (such as ACN) and was more environmental friendly. The POSS based MIPs columns can be used for the separation of racemate drugs and amino acids. Furthermore, for amino acids that with ultraviolet absorption, the derivatization with dansyl chloride is not needed. The optimum polymerization (c3) was prepared by mixing HP-β-CD, MA0735, MAA, and MBA with the molar ratio of 1 : 1.87 : 1.60 : 1.60. Higher resolutions of the enantiomers were obtained in the MIPs-POSS coating capillary, which was about 3.36 times than that of the POSS-free column. Under the optimum CEC conditions, DL-Phe obtained baseline separation with R_s of 6.15.

Conflicts of interest

The authors declare no conflict of interest.

Acknowledgements

The authors sincerely thank Professor Xu Xu (School of Chemistry and Environmental Engineering, Shanghai Institute of Technology, China) and Dr Wenjing Li (School of Pharmacy, Xi'an Medical University, China) for their help in the characterization of the coating materials. This work was financially supported by the National Natural Science Foundation of China (81202492), the Science Foundation of Shaanxi Province Science and Technology Department of China (2021SF-323), the Service Local Foundation of Shaanxi Province Department of Education of China (19JC035), and Science Foundation of Xi'an Medical University of China (2018XNRC03).

References

1 T. Yu, Y. Du and B. Chen, *Electrophoresis*, 2011, **32**, 1898–1905.
2 W. Li, G. S. Ding and A. N. Tang, *RSC Adv.*, 2015, **5**, 93850–93857.
3 C. Liu, J. Zhang, X. Zhang, L. Zhao and S. Li, *Microchim. Acta*, 2018, **185**, 227.
4 Z. S. Gong, L. P. Duan and A. N. Tang, *Microchim. Acta*, 2015, **182**, 1297–1304.

5 L. Escuder-Gilabert, Y. Martin-Biosca, S. Sagrado and M. J. Medina-Hernández, *J. Chromatogr. A*, 2014, **1363**, 331–337.
6 I. Ali, Z. A. Al-Othman, A. Al-Warthan, L. Asnin and A. Chudinov, *J. Sep. Sci.*, 2014, **37**, 2447–2466.
7 C. Aydoğan, V. Karakoç and A. Denizli, *Food Chem.*, 2015, **187**, 130–134.
8 C. Aydoğan and A. Denizli, *Anal. Biochem.*, 2014, **447**, 55–57.
9 L.-L. Fang, P. Wang, X.-L. Wen, X. Guo and X.-J. Guo, *Talanta*, 2017, **167**, 158–165.
10 A. Martín-Esteban, *Trends Anal. Chem.*, 2013, **45**, 169–181.
11 C. S. Scheve, P. A. Gonzales, N. Momin and J. C. Stachowiak, *J. Am. Chem. Soc.*, 2013, **135**, 1185–1188.
12 Y. Z. Zhang, J. W. Zhang, C. Z. Wang, L. D. Zhou, Q. H. Zhang and C. S. Yuan, *J. Agric. Food Chem.*, 2018, **66**, 653–660.
13 P. Luliński, J. Giebułtowicz, P. Wroczyński and D. Maciejewska, *J. Chromatogr. A*, 2015, **1420**, 16–25.
14 S. Yan, Y. Wang, Y. Jiang and W. Li, *Polymers*, 2016, **8**, 216.
15 W. J. Cheong, F. Ali, Y. S. Kim and W. J. Lee, *J. Chromatogr. A*, 2013, **1308**, 1–24.
16 Z. J. Tan and V. T. Remcho, *Electrophoresis*, 1998, **19**, 2055–2060.
17 Z. H. Wei, L. N. Mu, Y. P. Huang and Z. S. Liu, *J. Chromatogr. A*, 2012, **1237**, 115–121.
18 C. Kulsing, R. Knob, M. Macka, P. Junor, R. I. Boysen and M. T. Hearn, *J. Chromatogr. A*, 2014, **1354**, 85–91.
19 H. M. Omranipour, T. S. A. Sajadi, R. Kowsari, M. S. Rad and S. A. Mohajeri, *Curr. Drug Delivery*, 2015, **12**, 717–725.
20 I. Morelli, V. Chiono, G. Vozzi, G. Ciardelli, D. Silvestri and P. Giusti, *Sens. Actuators, B*, 2010, **150**, 394–401.
21 F. Svec, *J. Sep. Sci.*, 2005, **28**, 729–745.
22 Y. K. Lu and X. P. Yan, *Anal. Chem.*, 2004, **76**, 453–457.
23 L. J. Yan, Q. H. Zhang, J. Zhang, L. Zhang, T. Li, Y. Feng, L. Zhang, W. Zhang and Y. Zhang, *J. Chromatogr. A*, 2004, **1046**, 255–261.
24 H. Lin, J. Ou, Z. Zhang, J. Dong and H. Zou, *Chem. Commun.*, 2013, **49**, 231–233.
25 K. Tanaka and Y. Chujo, *J. Mater. Chem.*, 2012, **22**, 1733–1746.
26 K. Tanaka, F. Ishiguro and Y. Chujo, *J. Am. Chem. Soc.*, 2010, **132**, 17649–17651.
27 X. Lin, N. Zheng, J. Wang, X. Wang, Y. Zheng and Z. Xie, *Analyst*, 2013, **138**, 5555–5558.
28 M. Li, X. Lei, Y. Huang, Y. Guo, B. Zhang, F. Tang and X. Wu, *J. Chromatogr. A*, 2019, **1597**, 167–178.
29 Q. L. Zhao, J. Zhou, L. S. Zhang, Y. P. Huang and Z. S. Liu, *Talanta*, 2016, **152**, 277–282.
30 B. Zhang, X. Lei, L. Deng, M. Li, S. Yao and X. Wu, *Microchim. Acta*, 2018, **185**, 318–326.
31 M. Deng, S. Li, L. Cai and X. Guo, *J. Chromatogr. A*, 2019, **1603**, 269–277.
32 Z. Wang, H. Guo, M. Chen, G. Zhang, R. Chang and A. Chen, *Electrophoresis*, 2018, **39**, 2195–2201.
33 W. A. Wan Ibrahim, S. M. Abd Wahib, D. Hermawan and M. M. Sanagi, *Chirality*, 2013, **25**, 328–335.
34 C. Aydoğan, *Chirality*, 2008, **30**, 1144–1149.
35 A. Majid and S. H. Asadi, *Drug Test. Anal.*, 2012, **5**, 461–467.
36 X. Li, H. Wang, J. T. Robinson, H. Sanchez, G. Diankov and H. Da, *J. Am. Chem. Soc.*, 2009, **131**, 15939–15944.
37 S. Taira, D. Kaneko, Y. Kawamura-Konishi and Y. Ichiyanagi, *J. Nanosci. Nanotechnol.*, 2014, **14**, 3155–3162.
38 X. Qi, W. Wei, J. Li, Y. Liu, X. Hu, J. Zhang, L. Bi and W. Dong, *ACS Biomater. Sci. Eng.*, 2015, **1**, 1287–1299.
39 Z. H. Wei, X. Wu, B. Zhang, R. Li, Y. P. Huang and Z. S. Liu, *J. Chromatogr. A*, 2011, **1218**, 6498–6504.
40 L. Xie, J. Guo, Y. Zhang and S. Shi, *J. Agric. Food Chem.*, 2014, **62**, 8221–8228.